ISSN 0145-8752, Moscow University Geology Bulletin, 2021, Vol. 76, No. 4, pp. 383–397.

Bitumens as a Cause of the Occurrence of the Low Electrical Resistivity Zones in the Basement Rocks of the West Siberian Plate

A. O. Khotylev[a, *], E. V. Kozlova[b, **], V. S. Belokhin[a, *], A. A. Maiorov[a, ****], T. G. Isakova[c, *****], N. V. Pronina[a, ******], G. A. Kalmykov[a, *******], and O. V. Khotylev[c, ********]**

[a] *Department of Geology, Moscow State University, Moscow, 119899 Russia*
[b] *Skolkovo Institute of Science and Technology, Moscow, 121205 Russia*
[c] *National Intellectual Development Foundation, Moscow, 119192 Russia*
**e-mail: akhotylev@gmail.com*
***e-mail: e.kozlova@skoltech.ru*
****e-mail: v.belokhin@oilmsu.ru*
*****e-mail: alex.yora@gmail.com*
******e-mail: isakova@oilmsu.ru*
*******e-mail: nvproncl@msu.ru*
********e-mail: gera64@mail.ru*
*********e-mail: hot63@mail.ru*

Received January 26, 2021; revised January 28, 2021; accepted January 29, 2021

Abstract—This work reports on the results of the studies of the material composition and physical properties of the basement rocks of the West Siberian Plate. It has been shown that the rocks contain bitumens of anthraxolite and kerite groups. We assume that the bitumens create the Late Paleozoic paleodeposit, transformed under the conditions of apocatagenesis. Impregnation with highly transformed organic matter leads to a significant decrease in electrical resistivity to values of 1–30 ohm m, which must be taken into consideration when interpreting the low-resistivity zones on the basis of log data.

Keywords: electrical resistivity, bitumen, pre-Jurassic basement, Rock-Eval pyrolysis, low resistance collectors, Western Siberia

DOI: 10.3103/S0145875221040062

INTRODUCTION

The need to determine the causes of low electrical resistivity (ER) of rocks has arisen during the study of the cores of metasedimentary rocks from several wells, which had been drilled in one of the fields of the Krasnoleninsk arch in the central part of Western Siberia. The wells were located 120 km northwest of Khanty-Mansiysk, in the Oktyabr'sk and Khanty-Mansiysk raions of the Khanty-Mansiysk Autonomous Okrug–Yugra.

When interpreting the geophysical well logging, the low-resistivity intervals were defined as water-saturated fractured or brecciated zones. However, this interpretation was not confirmed by the studies of rock material. The core is represented by massive and poorly fractured metamorphic rocks, which are characterized by low porosity and permeability. Obviously, we should have expected that the ER would be controlled by the rock composition. Thus, the purpose of our study was to establish the cause of the low ER of the rocks in the eastern part of the Krasnoleninsk arch.

The direct source of information on a structure of oil-and-gas-bearing basins is the data on the core material obtained by drilling. However, in many cases, core samples are not taken or are taken fragmentarily. Therefore, the data of geophysical studies of wells become very important. Geophysical logging data are used to correlate strata, to determine geological boundaries, to assess water and oil saturation of rocks, and to evaluate the prospects of certain horizons in terms of oil production.

ER is one of the most important geophysical parameters. In sedimentary rocks, it is used in combination with other techniques (gamma-ray logging, neutron logging, spontaneous polarization, etc.) to identify lithotypes, such as carbonatized sandstones, clays, dense limestones, or dolomites. In addition, ER reflects fluid saturation (with hydrocarbons or aqueous solutions) of intergranular reservoirs, in which the pore volume is filled with fluid. The distinction on the basis of a fluid type is made due to the significantly higher ER (or low conductivity) of hydrocarbons

(HCs) compared to mineralized stratal waters. In the base case, the low resistivity zones are considered as water-saturated strata; the high-resistivity intervals are promising oil-saturated zones. However, in the late 1980s, the problem of the low-resistivity intergranular reservoirs was revealed when, according to geophysical surveys of wells, the Jurassic oil-saturated reservoirs in Western Siberia were designated as unpromising and water saturated (Ezhova, 2006; Gusev, 2016; Mel'nik, 2018).

It has been repeatedly shown based on the examples of sedimentary formations that resistance of rocks depends on some factors. The most common and important of them include:

—the amount, the pattern of distribution, and the composition of clayey minerals;

—the specific features of diagenetic and catagenetic transformations of rocks, the presence of low-resistivity minerals;

—the character and degree of rock fracturing;

—the type of the fluid filling of pores and fractures;

—the size and configuration of pores;

—the structure and texture of rocks;

—the orientation of rock textures (most often, layering) in relation to a well or the direction of measurement;

—the mineralization of stratal waters.

Low-resistivity nonclay phases that lower ER are titanium oxides, sulfides (pyrite, pyrrhotine, and chalcopyrite), hydroxides of iron-bearing minerals, and crustified chlorites.

However, the influence of these phases depends significantly on the amount: for pyrite, the lower limit is at 5–7% (according to different sources), below which it does not have a significant impact on the ER. The influence of the above factors was considered in detail in (Ezhova, 2006; Gusev, 2016; Mel'nik, 2018; Mel'nik and Erofeev, 2014; Semenov et al., 2006) and in the references in them.

Oil saturation is less common in the basement rocks; therefore, the nature of the low-resistivity zones in these rocks has been studied more poorly. In metamorphic and metamorphosed rocks, a pore reservoir is usually absent and the resistivity methods generally reflect the electrical properties of rocks themselves and depend to a greater extent on the mineral composition and structural-textural features of the deposits.

A fractured reservoir, which usually occurs in the basement rocks, has a porosity

of less than 1% and can be reflected in the ER data in different ways; this depends not only on the type of fluid saturation, but also on the properties and composition of dense and unfractured host rocks. In this particular case, there is no an unambiguous solution to the problem of the type of fluid in the fractured reservoirs.

In the base case, the low-resistivity zones in the basement are considered as the intervals of tectonic brecciation or the fractured reservoir zones filled with mineralized water. Initially, we believed that the occurrence of low-resistivity intervals in the studied wells was related to the fracturing and water saturation, whereas the share and features of the composition and distribution of clayey minerals (which are usually uncommon in the basement rocks) play a lesser role.

THE STUDY AREA

The study area is located in the central part of the Krasnoleninsk arch of the West Siberian plate, which has a complex and heterogeneous structure. Three structural floors are distinguished in the structure of the West Siberian plate (Surkov and Zhero, 1981; Western Siberia, 2000):

—the folded basement, which includes the Riphean–Paleozoic sedimentary, metamorphic, and magmatic formations;

—the intermediate rift-related floor, composed of the Late Permian and Early Triassic basalts and rhyolites, replaced up the section by the Medium-and Upper Triassic terrigenous formations. The stratigraphic extent of this complex varies in the West Siberian Plate;

—the plate cover, as represented by the Mesozoic–Cenozoic, almost undislocated sedimentary formations.

The two lower structural floors represent the pre-Jurassic basement or the pre-Jurassic plate complex. The lower floor is the basement and the second (intermediate) floor is the transitional complex between the folded basement and the undeformed formations of the sedimentary cover.

In the northeastern part of the basement of the Krasnoleninsk arch, the Late Cambrian metamorphic formations occur (Shadrina, 2018). They are represented by quartzites and biotite–muscovite–quartz shales (Fig. 1). The southern and western parts are composed of poorly metamorphosed terrigenous-sedimentary mylonitized formations, represented by metasandstones, metasiltstones, and, to a lesser extent, sericite–hydromica shales.

According to our data, to the west, in the area of the Em-Egovskaya uplift, there are the members of volcanics with the contrast composition that lie within these terrigenous–sedimentary formations. To the south, the terrigenous–volcanic formations were also described in the South Yelizar Trough. All these terrigenous–sedimentary and terrigenous–volcanogenic formations are dated the Devonian–Carboniferous on the basis of a few fauna findings (Bochkarev and Brekhuntsov, 2015; Chuvashov, 2009; Tugareva et al., 2018). The above-mentioned sedimentary and metamorphic formations are intruded by several large gran-

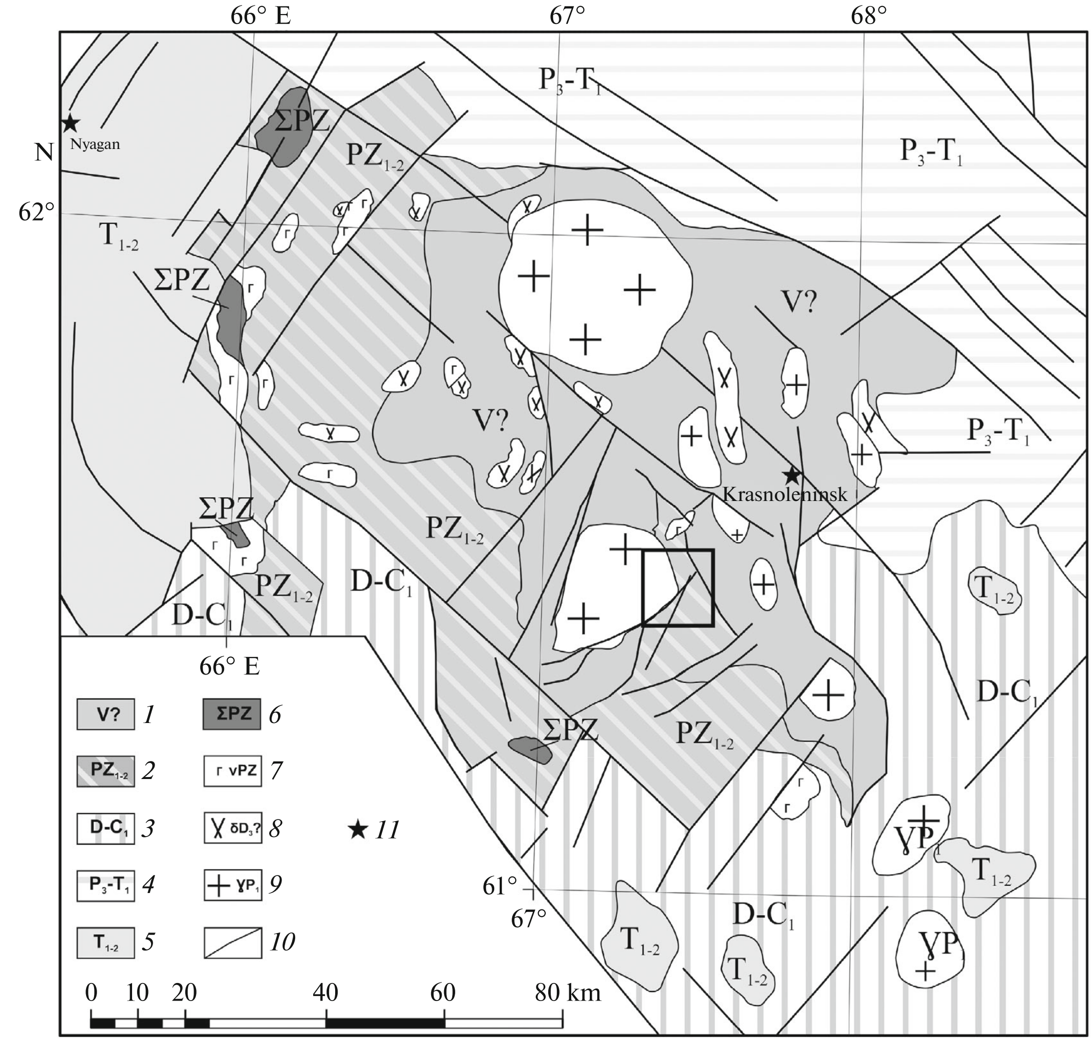

Fig. 1. The geological map-scheme of the basement structure of the Krasnoleninsk arch according to (Ivanov et al., 2016; Shadrina, 2018), with the author's additions and modifications. The study area is shown as a square: (*1*) the Vendian (?) Lower Paleozoic quartzites and mica shales; (*2*) the Lower-Middle Paleozoic metaterrigenous formations; (*3*) Devonian, Carboniferous terrigenous, carbonate, and volcanogenic complexes; (*4*) the Upper Permian, Lower Triassic volcanogenic Rogozhnikovskaya formation; (*5*) Lower-Middle Triassic volcanites of the Turin series; (*6*) bodies of the Paleozoic ultrabasites; (*7*) bodies of the Paleozoic gabbro and dolerites; (*8*) bodies of the Late Devonian (?) diorites; (*9*) massifs of granites and granodiorites of the Lower Permian complex; (*10*) faults; (*11*) settlements.

ite-granodiorite massifs of the Early Permian age (Fedorov et al., 2006; Ivanov et al., 2018), and small intrusions, presumably of the Late Devonian age, on the Em-Egovskaya uplift (Khotylev et al., 2021). From the northwest and northeast, the Krasnoleninsk arch is bounded by the Yuzhno-Bobrikovskii mega-trough, as well as the Yelizarovskii trough and Rogozhnikovskii swell, respectively, where the Triassic and Permian–Triassic volcanic complexes occur (Bochkarev et al., 2013; Shadrina and Kondakov, 2014).

MATERIALS AND METHODS

Our main purpose was to determine which of the rock parameters control the ER. Therefore, to show the relationship between the ER of the rocks and their composition and structural–textural features, we used data on the mineral composition and filtration-volumetric properties of the rocks as well as the information on the amount and the state of organic matter (OM) revealed in the rocks.

To determine the mineral composition of rocks, thin sections were studied and X-ray phase analysis (63 samples) was performed. ER of several types was measured on cylindrical samples including the resistivity of the 100% water-saturated samples with mineralization of 17 g/L (109 samples), the resistivity at residual water saturation (89 samples), and the resistivity of the samples dried at 80°C for 14 days (29 samples). To estimate porosity and permeability, we used the values of the coefficients of porosity (K_p, 114 samples) and permeability with a Klinkenberg correction (K_{per}, 85 samples), as obtained by the gas-volumetric method. The amount of organic matter was calculated on the basis of the Rock-Eval pyrolysis data; the total organic carbon content (TOC), which reflects the amount of organic carbon (C_{org}) in the rock in wt % (37 samples) was used for correlations.

The most complete complex of the studies was carried out on the samples from two wells (Wells A and B). This complex included the X-ray phase analysis, ER, pyrolysis, study of thin sections, and the determination of porosity and permeability. In addition, we used data on the ER, mineral composition, and filtration-volumetric properties of a number of rock samples from wells located in the same area.

The mineral composition of the rocks was determined by the X-ray phase method on a DRON-3M instrument at the Department of Oil and Gas Sedimentology and Marine Geology, Moscow State University (analyst V.L. Kosorukov).

The porosity (K_p) and permeability (K_{per}) of the samples were measured by the gas-volumetric method on the AP-608 equipment under laboratory conditions (confining pressure 500 PCI); nitrogen was used as a working fluid.

The ER of the samples was measured according to GOST25494-82 on the PetroOm equipment (Ecogeosprom, Russia). The samples were clamped by a core holder at the same pressure for all samples. When measuring the ER of dry samples, no auxiliary spacers were used between the sample and the electrodes. Filter paper pads moistened with mineralized water were used when measuring fully or partially saturated samples (mineralization corresponded to mineralization of sample saturation was 17 g/L).

To create of the residual water-saturation, we used the method of a semipermeable membrane on a group capillarimeter unit. This concept makes it possible to preserve the samples, unlike the method of centrifugation.

The general scheme of work with samples had the following stages:

(1) drilling, facing, washing, and drying (at 102°C to constant weight);

(2) measuring porosity and permeability to gas;

(3) saturation of a sample with mineralized water (mineralization 17 g/L);

(4) measuring the ER of a saturated sample;

(5) creation of the residual saturation of a sample by the semipermeable membrane method;

(6) estimation of the coefficient of residual water saturation by the weight method;

(7) measuring the ER on samples at residual saturation;

(8) drying the samples within 14 days at 80°C;

(9) measuring the resistivity of dry samples.

The entire cycle of described measurements was carried out in the laboratory of the Department of Geology and Geochemistry of Fuel Minerals, Moscow State University. Table 1 demonstrates the results of the determination of the ER and filtration-volumetric properties for the most representative samples.

The characteristics of the organic matter in the studied rocks were obtained by Rock-Eval pyrolysis on the Rock-Eval-6 instrument (Vincitechnology, France) and HAWK workstation (Wildcattechnology, United States) according to the standard temperature programs of *bulk rock* and *reservoir* (Kozlova et al., 2015; Lafargue et al., 1994; Lopatin and Emets, 1987). The total amount of organic carbon (TOC) was determined in rocks by the amount of thermally desorbed hydrocarbons HC (S_0, gaseous; S_1, light oil; S_2a, heavy oil; S_2b, asphaltenes and products of kerogen cracking (Batalin and Vafina, 2013)) and CO and CO_2, released upon heating and combustion (S_3 and S_4). The temperature ranges of the reservoir program were used to separate light and heavy oil parts in HC. To separate asphaltenes and kerogen cracking products, we carried out the extraction with chloroform in the Soxhlet apparatus and performed repeated pyrolysis for several samples (Table 2). The elemental composition of organic matter (CHN) was determined on an LECO instrument (CHNS 260 elemental analyzer, LECO, United States). The studies were carried out in the Center of Hydrocarbon Recovery of Skolkovo, Institute of Science and Technology; the results of the studies are given in Table 3.

Raman spectroscopy was carried out to clarify the composition of organic matter on the transparent-polished thin section. Raman spectra were obtained using an the XPloRA Raman spectrometer (HoribaScientific, Japan) coupled with a confocal microscope (Moscow State University, Department of Geology, Laboratory of Local Methods for Study of Matter, analyst V.D. Scherbakov) under excitation radiation with a wavelength of 532 nm and power of ~12 mW. Registration was performed in the 100–3900-cm^{-1} range at parameters giving a spectral resolution of approximately 1 cm^{-1}.

RESULTS AND DISCUSSION

We studied rocks of the pre-Jurassic complex uncovered by Wells A and B in the central part of the Kamennaya uplift. These rocks presumably belong to the Devonian–Carboniferous terrigenous-sedimentary formations. As mentioned above, we measured the ER and filtration properties of these rocks, determined their mineral composition, and carried out pyrolytic studies.

The lithological characteristics of the rocks. The upper part (interval 2278.0–2289.5 m) of Well A is composed of light brown, beige metasandstones, fine-grained, foliated, with calcite and dolomite stringers

Table 1. The values of the ER and filtration-volumetric properties for the rocks of the Krasnoleninsk arch

Parameter	Value	Metasiltstones, well 1A, 2B	Metasandstones, well 1A, 2B	Grano-diorites	Sericite-quartz shales	Sericite-hydromica-quartz shales
Number, n		14	7	29	11	19
$ER_{100\%}$, Ohm m	avg.	25	302	282	397	263
	min	0.2	67	55	202	76
	max	60	849	967	862	560
ER_{rws}, Ohm m	avg.	34	842	4029	2121	3927
	min	0.0005	100	111	352	377
	max	85	1713	19000	3940	18675
K_p	avg.	2.557	0.454	1.92	1.03	1.25
	min	0.62	0.02	0.657	0.302	0.314
	max	8.136	1.748	5.302	2.249	3.067
K_{per}, mD	avg.	0.048	0.054	–	0.086	0.024
	min	0.001	0.001	–	0.001	0.001
	max	0.551	0.106	–	0.611	0.261

$ER_{100\%}$, resistivity at 100% water saturation; ER_{rws}, resistivity at residual water-saturation; K_p, coefficient of porosity, K_{per}, coefficient of permeability.

and pegmatite veinlets of black quartz. The metasandstones contain dark gray to black quartz-sericite carbohydrate shales up to 30-cm thick.

In the lower part (2385–2395 m), the metasandstones are represented only by single members up to 20-cm thick; dense dark gray thin-layered tectonized metasiltstones predominate (Fig. 2, a, b). The rocks are penetrated by numerous quartz veins, dislensing with plicated textures; the incidence angle of foliation varies from 50 to 90° (horizontal) to the core axis.

The basement rocks with the structural unconformity are overlain by the Jurassic coarse-clastic conglomerates with a sandy matrix and carbonate cement. Below the contact, weathering processes are developed: bleaching, fracturing, disintegration of the basement rocks, development of iron oxides, and the formation of quartz caverns.

Metasandstones are fine- and fine-grained, poorly rounded, basically quartz with mica-quartz fine-grained cement. The texture is nonlayered, often breccia, tectonized. Debris are represented by angular quartz grains with wavy and blocky extinguishment (0.1–0.3 mm, 15–20%), with single similar-sized plagioclase fragments and microquartz fragments. The clastic component is in a matrix; it is composed of thin quartz fragments (0.08–0.02 mm, 30–40% of rock), sericite and hydromica leaflets (0.04–0.08 mm, 10–15%), and single leaflets of muscovite (up to 0.16 mm). The rock contains uneven, lenticular, poured, and swollen veinlets of granulated quartz and fine-crystalline calcite (0.1–1 mm, up to 5–8%) (Fig. 2, c, d). Rhombic pyrite porphyroblasts of up to 1–1.2 mm were observed. The organic matter is fine, dust-like or in the form of small slices (no more than 0.1%).

The metasiltstones are thin-banded lepido-granoblastic fine-microcrystalline sericite—quartz shales, impregnated with black isotropic organic matter. The texture of the rocks is lenticular, plicated, microfolded, and modified by isolated quartz phenocrysts, which create a porphyroblast or even almost rare-augen structure. The rocks are composed of sericite leaflets of less than 0.005 mm (up to 70–75%) and granoblastic quartz crystals (up to 15%), which form 0.5–5 mm lens-like clusters (Fig. 2, a, b). The banded structure of rocks is caused by the presence of lenses of light quartz and strips enriched in black organic matter. These bands are up to 0.5-mm thick; they account for up to 40% of the rock, but there are no visible differences in their mineral composition (except for organic matter).

Organic matter is represented by numerous lenticular stringers and veinlets that are 0.01–0.05-mm thick and 0.5–6 mm and more in length, which are oriented along the foliation and transverse to the foliation on ptygmatite veinlets; visually, it ranges from 1–2 to 10–12%.

The rocks uncovered by Well B in the entire studied interval (2372–2412 m) are represented by mylonitized fine-grained terrigenous formations: metasandstones, meta siltstones, and metaclaystones. Metasiltstones fine-grained, grano-lipido-blastic, which are indistinctly banded to foliated, predominate.

The texture strongly depends on the degree of mylonitization and varies from homogeneous, very indistinctly banded to foliated and lenticular-banded. Plication is very common, thin quartz veinlets deformed into ptygmatite folds are sometimes encountered. The rocks are folded, which is clearly

Table 2. Data from the pyrolytic study

Sample number	Depth, m	Lithology	S_1+S_{2a} oils and resins mg HC/g rock	S_{2b} asphaltens of kof kerogene, mg HC/g rock	S_3, mg CO_2/g rock	T_{max}, °C	TOC, wt %	HI, mg HC/g TOC	OI, mg CO_2/g TOC	PC, wt %	RC, wt %	CC, wt %	NSO, mg/g rock	Bitumen, mg/g rock
13A	2278.06	Metasandstones fine-grained	0.11	0	0.08	–	0.1	90	80	0.01	0.09	0.7	1	1.11
1A	2280.07	Metasiltstones	1.17	0.57	0.16	–	0.33	258	48	0.16	0.17	8.69	2.46	3.63
14A	2280.27	Metasiltstones	1.79	0.88	0.05	415	0.4	250	12	0.23	0.17	7.53	2.77	4.56
15A	2285.63	Metasandstones	0.05	0.03	0.03	–	0.11	36	27	0.02	0.09	0.25	1.03	1.08
16A	2288.8	Metasandstones	0.03	0.02	0.05	–	0.21	10	24	0.01	0.2	0.32	2.24	2.27
17A	2289.01	Metasandstones coarse-grained	0.02	0.01	0.04	–	0.23	9	17	0	0.23	0.05	2.57	2.59
2A	2289.08	Metasandstones	0.03	0.01	0.07	–	0.04	50	175	0.02	0.02	0.93	0.24	0.26
18A	2294.7	Metasiltstones	0.05	0.02	0.04	–	0.06	67	67	0.01	0.05	0.33	0.58	0.63
19A	2297.23	Metasandstones	0.46	0.22	0.01	486	0.33	118	3	0.07	0.26	1.36	3.11	3.57
4A	2385.2	Metasiltstones	0.05	0	0.03	–	1.7	1	2	0.04	1.66	0.26	18.44	18.49
3A	2385.26	Metasiltstones carbonaceous	0	0.01	0.04	487	0.31	3	13	0	0.31	0.07	3.45	3.45
5A	2385.8	Metasandstones medium-grained	0	0.02	0.04	486	0.35	6	11	0.01	0.34	0.13	3.8	3.8
6A	2385.9	Metasiltstones	0.05	0	0.02	–	1.67	1	1	0.02	1.65	0.62	18.33	18.38
7A	2386.26	Metasiltstones	0.05	0	0.02	–	0.81	4	2	0.01	0.8	0.23	8.89	8.94
8A	2387.85	Metasiltstones	0	0	0.01	–	0.15	0	7	0.01	0.14	0.14	1.56	1.56
9A	2388.35	Metasiltstones carbonaceous	0.03	0	0.02	–	0.77	1	3	0.01	0.76	0.08	8.44	8.47
10A	2389.7	Metasandstones	0	0.01	0	494	0.4	2	0	0.01	0.39	0.2	4.34	4.34
11A	2390.79	Metasiltstones	0.02	0	0	–	0.4	2	0	0.01	0.39	0.14	4.33	4.35
12A	2391.56	Metasiltstones	0.01	0	0	–	0.35	0	0	0.02	0.33	0.08	3.67	3.68
1B	2369.37	Metasiltstones carbonaceous	0.03	0.02	0.18	–	0.15	13	120	0.01	0.14	3.46	1.57	1.61
2B	2372.73	Metasiltstones	0.04	0.02	0.06	–	0.6	5	10	0.01	0.59	0.13	6.58	6.62
3B	2372.75	Metasiltstones	0.31	0.16	0.25	–	0.88	28	28	0.05	0.83	5.68	9.38	9.69
4B	2373.11	Metasiltstones carbonaceous	0.18	0.09	0.06	–	0.5	22	12	0.02	0.48	0.51	5.42	5.6
5B	2374.4	Metasiltstones carbonaceous	1.09	0.54	0.07	454	4.71	18	1	0.14	4.57	0.05	51.32	52.41
6B	2374.73	Metasiltstones carbonaceous	0.82	0.41	0.04	–	2.89	20	1	0.1	2.79	0.06	31.41	32.23
7B	2376.04	Metasiltstones carbonaceous	1.59	0.78	0.13	–	1.73	103	8	0.2	1.53	0.12	17.78	19.37
8B	2376.48	Metasiltstones carbonaceous	0.23	0.11	0.03	–	0.75	19	4	0.03	0.72	0.02	8.11	8.34
9B	2376.55	Metasiltstones	0.05	0.02	0.02	–	0.11	27	18	0.01	0.1	0.02	1.13	1.18
10B	2377.63	Metasiltstones	0.24	0.12	0.01	–	0.33	42	3	0.03	0.3	0.02	3.45	3.69
1B	2408.08	Metasiltstones carbonaceous	0.31	0.15	0.1	–	1.76	13	6	0.04	1.72	0.15	19.26	19.57
12B	2408.73	Metasiltstones	0.22	0.11	0	–	1.73	10	0	0.04	1.69	0.24	18.89	19.11
13B	2409.72	Metasiltstones	0.18	0.09	0.02	446	1.51	10	1	0.02	1.49	0.17	16.64	16.83
14B	2409.93	Metasiltstones carbonaceous	0.33	0.16	0.06	447	2.52	11	2	0.04	2.48	0.2	27.72	28.05

TOC — organic carbon, PC — pyrolized carbon, RC — residual carbon, CC — mineral carbon. Samples 1A–13A — from Well 1A, samples 1B–14B — from Well 2B.

Table 3. The values of filtration-volumetric properties and ER of the studied rocks

Sample number	Well	Deph, m	K_p	K_{per}, mD	$ER_{100\%}$, Ohm m	ER_{rws}, Ohm m	ER_{dry}, Ohm m
1A	1A	2280.07	8.136	0.067	59.8391	161.52	542033.3
2A	1A	2289.08	1.748	0.041	172.4877	611.5773	1696800
3A	1A	2385.26	0.357	0.008	0.91	9.8833	1.227823
4A	1A	2385.2	0.365	0.106	0.792	8.2402	10.605
5A	1A	2385.8	0.28	0	67.7004	100.8948	123.9607
6A	1A	2385.9	0.289	0.001	0.2915	2.2445	1.649667
7A	1A	2386.26	0.259	0	0.2083	2.5953	1.649667
8A	1A	2387.85	0.214	0.001	781.1484	2955.29	131973.3
9A	1A	2388.35	0.341	0.024	9.7357	12.3104	13.90433
10A	1A	2389.7	0.365	0	80.6672	235.8468	136.6867
11A	1A	2390.79	0.281	0.001	849.7288	1713.427	1508267
12A	1A	2391.56	0.367	0.064	106.1032	117.968	148.47
1B	2B	2369.37	3.141	0.005	46.1951	74.6576	471333.3
2B	2B	2372.73	6.357	0.015	31.7647	45.6978	1767500
3B	2B	2372.75	2.285	0.003	–	4.3074	8.8375
4B	2B	2373.11	3.364	0.015	–	12.0792	16.16673
5B	2B	2374.4	4.636	0.004	20.1	0.0004	0.542033
6B	2B	2374.73	0.62	0	45	0.1012	0.8484
7B	2B	2376.04	4.557	0.005	–	0.4356	1.178333
8B	2B	2376.48	3.031	0.001	–	6.3657	5.773833
9B	2B	2376.55	2.996	0.003	43.3048	68.3845	106050
10B	2B	2377.63	4.858	0.007	48.6233	85.0124	54203.33
11B	2B	2408.08	0.576	0.002	38	0.0005	7.871267
12B	2B	2408.73	0.678	0.002	–	0.4674	3.417167
13B	2B	2409.72	0.62	0.008	1.94	4.0874	5.255367

K_p, coefficient of porosity; K_{per}, the coefficient of permeability; $ER_{100\%}$, resistance at 100% water-saturated samples; ER_{rws}, resistance of the samples at residual water-saturation; ER_{dry}, the resistance of the dried samples.

visible in the change in the angle of foliation to a core axis from 90° (horizontal) to 40°.

The basement rocks with structural unconformity are overlain by various clastic conglomerates and pebble stones of Jurassic age. The weathering crust is developed under the contact, which is manifested in the rock bleaching and intense fracturing.

The basement rocks are homogeneous in composition; they are composed of an aggregate of granoblastic quartz (crystals are 0.008–0.05 mm) and leaflets of sericite and hydromica (0.008–0.04 mm) (Fig. 2, e, f). The grayish green chlorite, which forms lepidoblastic nests of no more than 0.1–0.15 mm, is detected. There is few pyrite among accessory minerals; it forms xenomorphic stringers along the foliation, which does not exceed 0.5 mm in length. The share of quartz ranges from 20–22 to 50–55%, that of mica is from 10–15 to 50%, chlorite is from 1–2 to 10–15%, and pyrite is no more than 1–3%. These variations are responsible for changes in the section from fine-grained quartz metasandstones with sericite to metasiltstones and, in some cases, to almost quartzless sericite–hydromica shales (metaclaystones).

The rocks are unevenly saturated with black isotropic organic matter; its share in thin sections is estimated from 0.1 to 35–40% (more than half of the field of view is not transparent). The organic-rich intervals are characterized by the most intense development of foliation and lenticular-banded textures; 50% of the studied interval (13 m) consist of such carbonaceous, organic-rich varieties.

In addition, we measured the physical properties (ER, K_p, and K_{per}) of the following metasedimentary and magmatic rocks of the basement from several wells of the Krasnoleninsk arch (Table 1):

—sericite–quartz shales with muscovite and biotite, chlorite and tourmaline, fine-thin-crystalline, lepidogranoblastic, thin-banded (11 samples);

—granodiorites, medium-fine-crystalline, massive (29 samples);

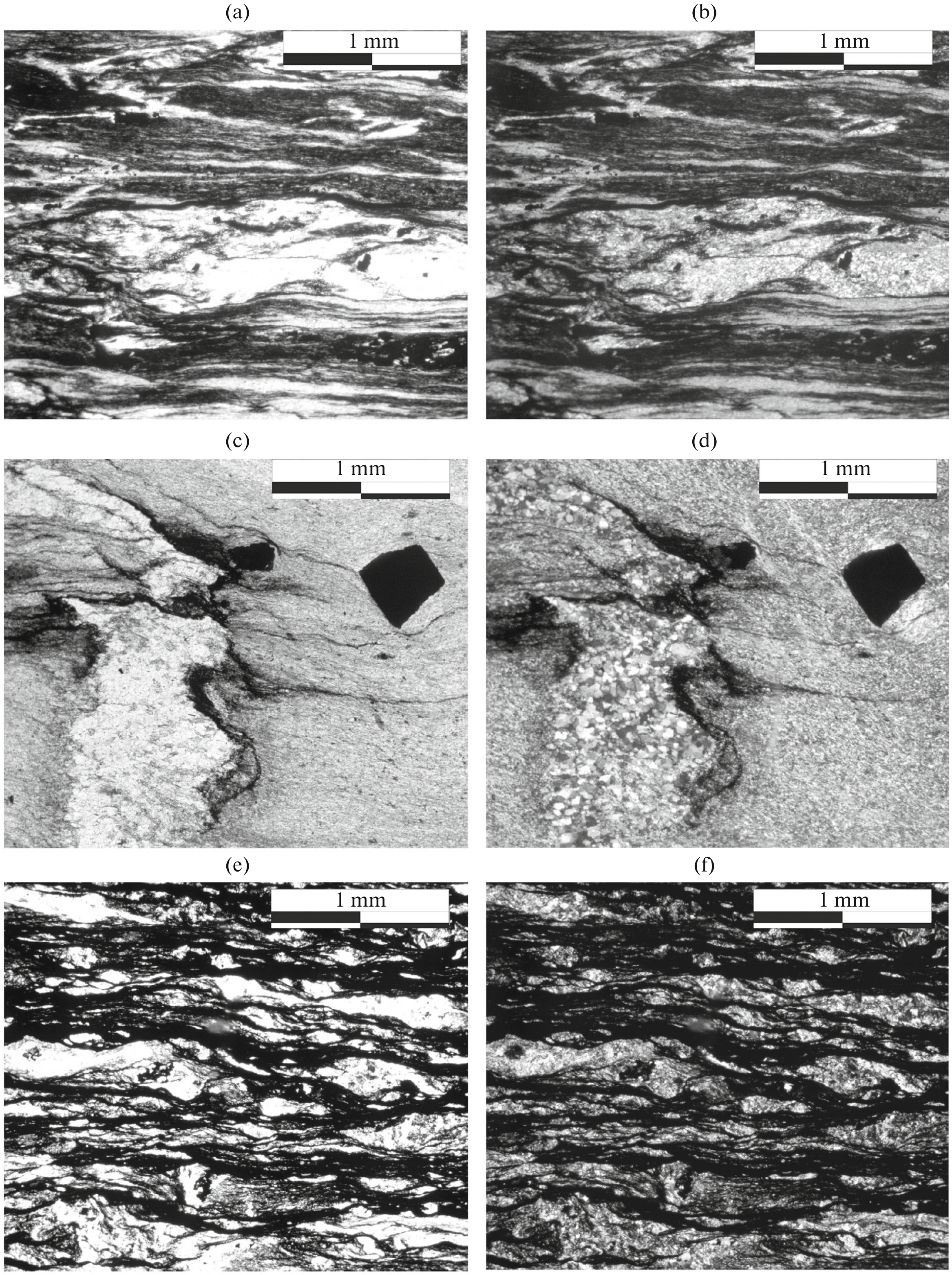

Fig. 2. Photos of thin sections of the studied rocks: (a, b) sandy siltstones with lenses of granoblastic quartz impregnated with black organic matter, sample 4A, Well A; (c, d) fine-grained sericite–quartz sandstones with a ptigmatite veinlet of granoblastic quartz and a large rhombic crystal of pyrite, sample 8A, Well A; (e, f) milonitized, lens-like banded sandy sericite–quartz siltstones, with stringers and veinlets of black organic matter, sample 5B, Well B; (a, c, d) without an analyzer; (b, d, f) with an analyzer.

—shales, sericite—hydromica—quartz granolepidoblastic, fine-crystalline, thin-banded, dense (19 samples).

These rocks do not contain organic matter; therefore, pyrolytic studies were not carried out on them.

The physical properties of the rocks. The resistivities of water-saturated samples (100% saturation) of metasandstones, sericite—quartz shales, and sericite—hydromica—quartz shales of the Krasnoleninsk arch are similar, ranging from 260 to 850 ohm·m. Granodiorites also have similar values, their $ER_{100\%}$ is 280—967 ohm m. The $ER_{100\%}$ of quartzites is slightly higher, ranging from 977 to 7077 ohm m. The metasiltstones are characterized by the lowest resistivity among all the studied rocks, ranging from 25 to 60 ohm·m at 100% water saturation. However, metasiltstones and metasandstones from Wells A and B have significantly lower resistivity at the residual water saturation than all other rocks (Table 1).

The rocks of the pre-Jurassic complex are characterized by lower porosity and permeability in comparison with the rocks of the sedimentary cover. In metasedimentary rocks, the coefficient of porosity ranges from 0.2 to 3—5 and averages 1—2%. The porosities of metasiltstones are slightly higher; K_p is up to 8.1%. Granodiorites are characterized by K_p values that are similar to metasedimentary formations and vary from 1.9 to 5.3%.

The permeability of the metamorphic rocks is extremely low, the coefficient of permeability for all studied samples does not exceed 0.62 mD; on average it is 0.05—0.1%.

The composition of the organic matter. To assess the composition of the organic matter, we analyzed a collection of 34 samples from two wells (Table 2).

Different characteristics were obtained for sandy and silty varieties for the samples from Well A. The sandstones have the lowest TOC values, up to 0.4 wt % (0.26 wt % on average), with a very small amount of hydrocarbons (<0.1 mg HC/g rock) extracted from the main mass. However, in the carbonatized varieties of sandstones, the level of $S_1 + S_2$ is up to 2.76 mg HC/g rock. The significant residual amount of C_{org} (RC) in sandstones indicates that the migrated HCs are preserved in them, whereas S_2 generally relates to heavy hydrocarbon compounds that boil out at a high temperature.

There is much more organic carbon in the dark gray metasiltstones, up to 1.67 wt %. This is mostly due to nonpyrolyzable residual carbon, which is determined in the oxidation stage of pyrolysis (Fig. 3). It is not possible to correctly determine the temperature of S_2 peak because of the low concentration of HC. In this case, this temperature will determine the melting point of the heavy oil fraction (presumably asphaltenes). However, we provided several values ranging from 486 to 494°C T_{max} for comparison with the samples from the second well in Table 2.

Among the samples from Well B, only carbonaceous metasiltstones were studied by pyrolysis. The TOC content here is much higher, varying from 0.11 to 4.71 wt % (1.44 wt % on average). Correspondingly, the TOC content increases and the pyrolyzed hydrocarbons reach 2.37 mg HC/g rock ($S_1 + S_2$) (Table 2).

The pyrograms also illustrate that oils dominate among HCs; the resinous-asphaltene components are detected by the double peaks of S_2a and S_2b (Fig. 4) (Batalin and Vafina, 2013). The main share of organic carbon is nonpyrolysable carbon (the pyrogram shows a large S_4 peak at the oxidation stage). T_{max} is 446—454°C. The S_1 and S_2 peaks decreased after extraction with chloroform; however, the maximum of the S_2 peak remained at the same temperature. According to a nearly four-fold change in the S_2 peak, soluble resinous-asphaltene components were in the sample as well (Fig. 5)

The electrical resistivity of the rocks. Initially, we made the most obvious hypothesis that ER will be controlled by the porosity and permeability of rocks due to saturation with conductive mineralized fluid. In fact, for the studied rocks, there is a clear relationship between resistivity and porosity; this is especially clear for water-saturated rocks: the increase in porosity from 0.2—0.3 to 10% leads to a decrease in ER from 10^3 to 10 ohm m (Fig. 6, a). The same plot demonstrates that resistivity of some samples with high porosity (5—10%) after drying increases by 3—5 orders of magnitude, from 10—100 to 105—106 ohm m. Obviously, the low resistance of these samples is controlled by water saturation. However, there are samples with low values of resistance (1—10 ohm m) and porosity (not more than 1%). The resisvity of these samples does not change during saturation with fluid and presumably depends on other factors.

The permeability results were less expected. When we initially interpreted the low-resistivity intervals as “brecciation intervals” by the GIS, we expected the rocks to be highly fractured and assumed their increased permeability. However, the permeability of the studied rocks does not exceed 0.6—0.8 mD and the expected negative relationship with ER values was not detected (Fig. 6, b).

Therefore, we suggested that the composition of the mineral matrix has an effect on ER . To clarify the relationship between the mineral composition of rocks and resistivity, we analyzed data on the quartz content (high-resistivity component), pyrite (low-resistivity component) and the sum of clay minerals (hydromica, chlorite, kaolinite, and mixed minerals of a montmorillonite group, the low-resistivity component). These components are rock forming and create the framework of the rocks. According to the results of X-ray diffraction analysis (XRD) and the study of thin sections of the rocks, we also encountered siderite, calcite, dolomite, gypsum, feldspars, tourmaline, and muscovite. However, these minerals are not men-

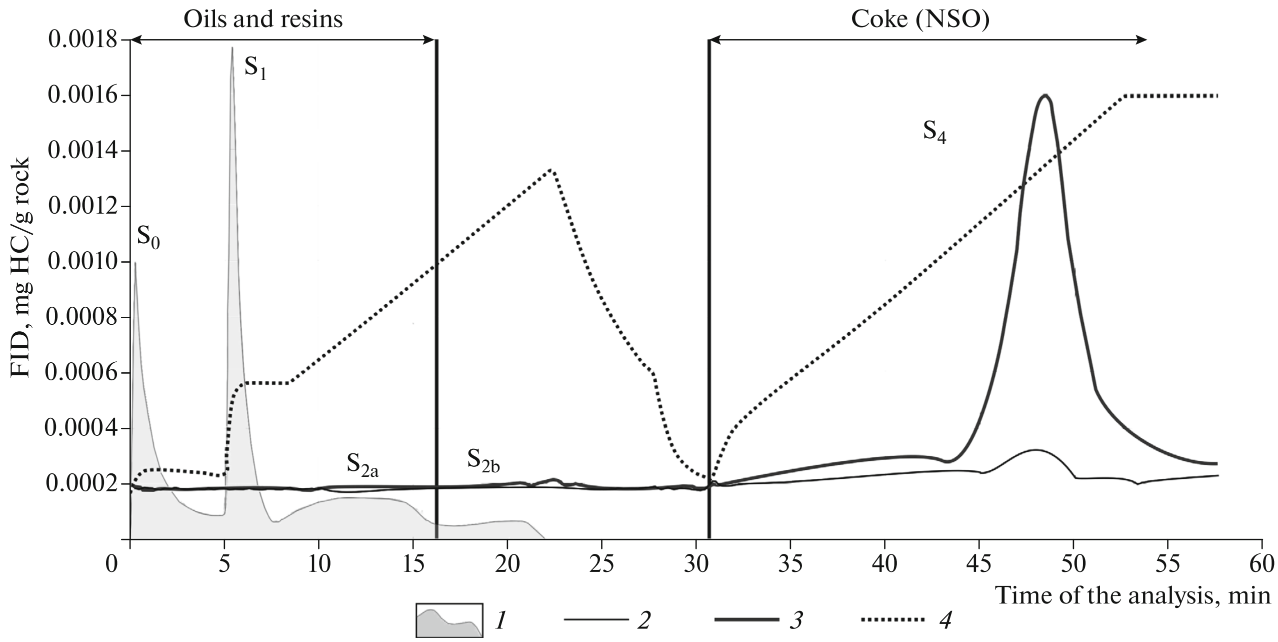

Fig. 3. The example of the pyrogram of the sample from Well A, depth 2388.35 m, sample 9A: (*1*) FID (flame ionization detector); (*2*) IR CO_2; (*3*) IR CO; (*4*) the furnace temperature.

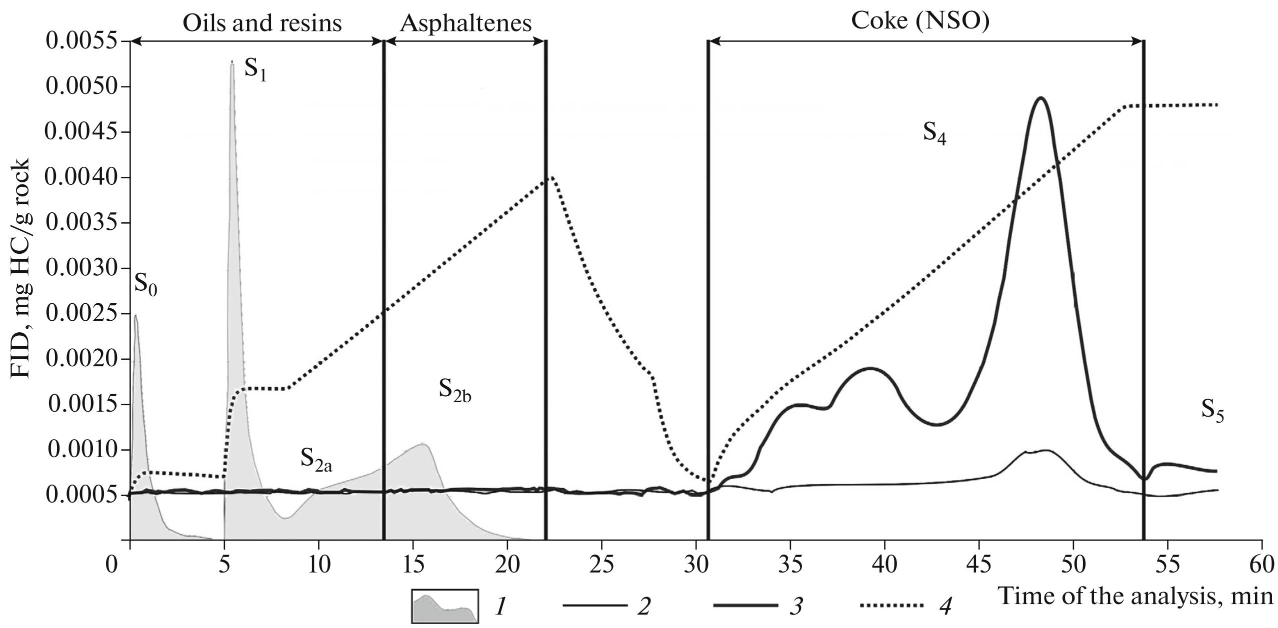

Fig. 4. An example of a pyrogram of the sample from Well B, depth 2374.73 m, sample 6B: (*1*) FID (flame ionization detector); (*2*) IR CO_2; (*3*) IR CO; (*4*) the furnace temperature.

tioned in further discussion, because they were found only in individual samples in insignificant amounts.

The amount of clayey minerals in the studied rocks actually has no effect on the ER of the rocks: no dependence of resistivity values on the amount of clay minerals was revealed (Fig. 6, c). Montmorillonites are characterized by the greatest sorption capacity among all clayey minerals, and therefore can significantly increase conductivity of rocks. Minerals of a hydromica group also increase conductivity of rocks (Mel'nik, 2018), while in the studied rocks, montmorillonites were not found at all, and the "hydromica", as determined by XRD, may be closer to sericites than to complete hydromica, which is confirmed by their optical characteristics in the thin sections.

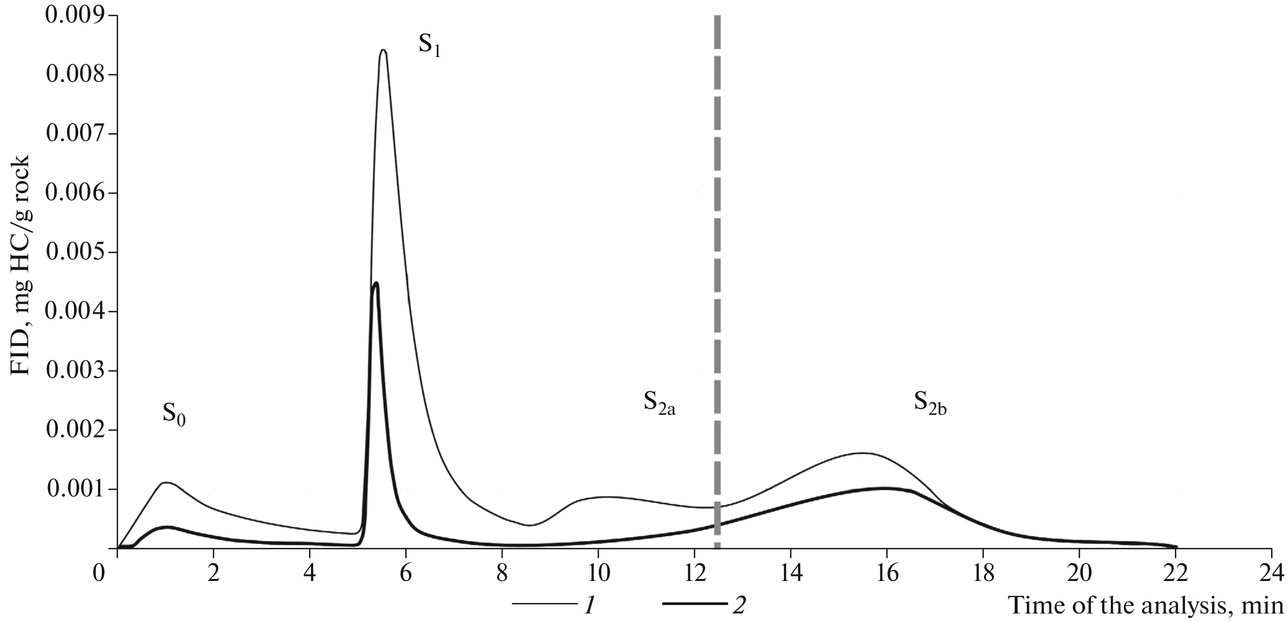

Fig. 5. The pyrogram of sample 5B from Well B before and after extraction: (*1*) before extraction; (*2*) after extraction.

As a result, this group of minerals does not contribute significantly to the increase in rock conductivity in unweathered metasedimentary formations of the basement.

No relationship was detected between ER and the pyrite content. In the samples where the amount of pyrite is more than 2–5%, the ER of all types remains the same as in the samples with pyrite below the detection limit, of less than 0.5% (Fig. 6, d). We believe that pyrite has no significant effect on conductivity because it forms lenticular stringers isolated from one another (this is clearly visible in the thin sections). The effect would be noticeable only if the stringers were in contact with each other and formed conductive veinlets and zones.

The quartz content has a poor positive relationship with the ER of the rocks: when the quartz content increased from 10 to 70–80%, resistivity increased by an order of magnitude (Fig. 6, f). This correlates well with the data of the studies of the thin sections: the highest resistivity values are determined in quartz sandstones and quartz siltstones with a low share of the sericite–hydromica matrix and dramatic predomination of the arkose component. The minimum values of resistivity were found in fine-grained siltstones with a large share of sericite–hydromica matrix and in metaclaystones.

The dependence of ER on the amount of organic matter was much more interesting (Fig. 6, e). As can be clearly seen, under a decrease of TOC from 0.1–0.2 to 5%, the ER of all types decreases by 3 orders of magnitude or more. In spite of the fact that there is a clear relationship between the filtration-volumetric properties and the rock resistivity (Fig. 6), the samples with the lowest ER are not the most porous (K_p is up to 0.7%) and have extremely low permeability values ($K_{per} < 0.01$ mD), i.e., these low values of resistivity are related specifically to the high content of organic matter and not to the filtration-volumetric properties, the amount of pyrite, the abundance of clay minerals, or other parameters.

This relationship is completely unexpected, because saturation with organic matter usually leads to an increase in resistivity, due to which oil- and water-saturated intervals are distinguished (see the review at the beginning of the paper). As an example, a clear positive dependence of ER on the amount of organic matter is known for the Bazhenov Formation (Skvortsov et al., 2018).

The revealed relationship is also confirmed by the data on the thin sections. Metasiltstones and fine-grained metasandstones with shaley lenticular-banded textures, filled with black untransparent organic matter, are most conductive (Fig. 2, a, b, and e, f). We believe that the increased conductivity is caused by the organic component of the rocks, which is represented by extended lenses and stringers, which often merging into single layers that provide conductivity throughout the entire rock volume. In principle, pyrite could also create such an effect, but its segregations are short and scattered and do not merge into single conductive systems. Thus, it was established that ER in the studied metasedimentary formations is regulated by porosity (increase in porosity–decrease in resistivity) due to saturation with aqueous conductive fluid, as well as by

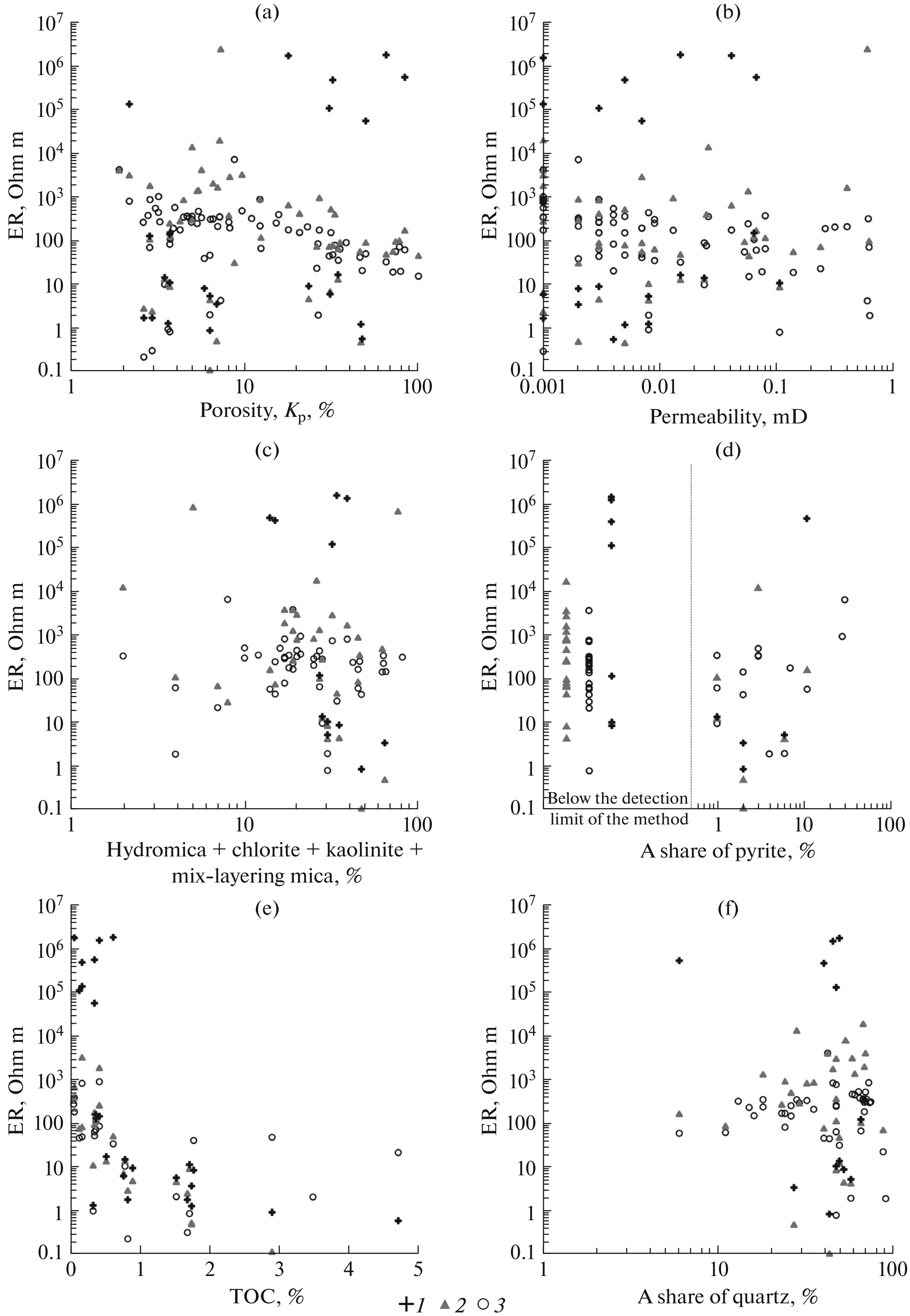

Fig. 6. The dependence of different types of ER on filtration-volumetric properties of rocks, the total amount of organic carbon (TOC), pyrite, quartz, and clayey minerals (wt %): (*1*) ER of rocks after drying; (*2*) ER of rocks at residual water-saturation; (*3*) ER of rocks at 100% water saturation.

the amount of organic matter (increase in the share of organic matter leads to a decrease in resistivity).

Combining the results of lithologic and pyrolytic studies allows us to state that the organic matter of the studied rocks is represented by natural pyrobitumen obtained during thermal reactions, which result in the removal of lighter hydrocarbons and in leaving an insoluble, carbon-rich residue. The pyrograms show very high temperatures of the coke combustion at the oxidation stage (S_4 peak), which are similar for the samples from both wells. According to the evaporation temperature among hydrocarbons, it is possible to extract oils and heavy parts of oil (preferably resins) in the low-temperature zone, and asphaltenes in the high-temperature zone (Fig. 3, 4). This was confirmed by duplicating the analysis using the reservoir program and separating the S_2 peak into S_2a and S_2b.

The metasiltstone samples from Well A are characterized by almost complete absence of the high-temperature S_2 peak (Fig. 2), which indicates a high degree of the transformation of organic matter. The bitumen can be diagnosed as “anthraxolite” affected by strong thermal processing (Filippov, 2013; Melenevskii et al., 2008].) This is confirmed by the fact that it could not be dissolved in chloroform, as well as an atomic H/C ratios equal to 0.48 (C, 3.95 wt %; H, 0.16 wt %; and N, 0.07 wt %.) The increase in the level of thermal transformation of organic matter is accompanied by an increase in the temperature $T_{\max}$. However, in the same well, in the upper part of the pre-Jurassic basement, carbonatized sandstones are saturated with hydrocarbons with a high hydrogen content. Apparently, the rocks in the upper part are not as heavily transformed. Bitumen from Well B contains a soluble portion and an insoluble residue, and apparently was not as affected by the thermal processing as the samples from Well A (Figs. 3, 4). The pyrolyzed part contains both a hydrocarbon component and heteroatomic compounds of an oil series, which are represented by soluble asphaltenes.

This bitumen is more appropriately called albertite (kerite) (Filippov, 2013) with a low content of the oil fraction and partial solubility in chloroform. The H/C atomic ratio is 0.95 (C, 4.4 wt %; H, 0.35 wt %, and N, 0.18 wt %).

Pyrolysis of heavy components of natural bitumen (mainly asphaltenes) is always accompanied by the formation of coke and the amount of bitumen in mg/g of rock can be estimated by the amount of released HC, CO, and CO_2 (Table 2). The maximum amount among the samples of the studied rocks (52 mg of bitumen/g of rock) was determined in well B.

Thus, according to the pyrolysis data, anthraxolite and albertite (kerite) bitumens were revealed in both wells, which indicates a sufficiently high transformation of organic matter. Bitumens are partially soluble in organic solvents; however, their main part is represented by a black carbonaceous substance, that is, solid oil coke, which was affected by significant thermal processing. The insoluble bitumen from the metasiltstones of Well A is represented by anthraxolites, which were transformed to the apocatagenesis stage and have almost no hydrogen. The organic matter from the sediments uncovered in Well B was least transformed. The degree of catagenesis of these bitumens, as represented by kerites, most likely can be estimated at the level of MK_3–MK_4.

A high degree of transformation of organic matter was detected by optical methods as well. In crossed nicols, organic matter is not black and isotropic, as it should be in an unstructured state, but it is finely scaly with extinguishing of individual scales. The disappearance of the optical isotropy of substance is caused by gradual ordering of a structure during heating, which provides conductivity. The limiting case of further transformation of organic matter will be graphite with a tabular value of ER of 8×10^{-6} ohm m. However, even transformation to the anthraxolite stage leads to a significant decrease in ER values; for the Shunga anthraxolite, it is 2.18×10^{-4} ohm m (*Shungity*..., 1975).

The organic matter is partially transformed into graphite, which is confirmed by the Raman spectroscopy data. We obtained reproducible spectra with intense lines with the centers at 1347, 1584, and 2697 cm^{-1} in different grains (Fig. 7), which correspond to graphite (Reich and Thomsen, 2004).

Oil cracking, which could lead to the formation of such bitumens, occurs under the natural conditions, when the temperature rises to at least 150°C, for example, due to heating of an intrusive body (Melenevskii et al., 2008). We assume that the decrease in the degree of transformation of organic matter in the rocks of Well A from bottom to top could be attributed to the thermal impact of the Kamennyi large granite pluton, which is located nearby (Melenevskii et al., 2008).

The studied rocks show alternation of relatively coarse-grained metasandstones and fine-grained metasiltstones, which are unevenly saturated with carbonaceous matter. The studied bitumens are the product of the transformation of primary organic matter contained in siltstones and finer-grained varieties that were the oil source rocks. The attribution of organic matter to the fine-grained metasiltstones and metaclaystones indicates that organic matter in the rocks was primary-sedimentary (rather than represented by hydrocarbons, that migrated from outside). If hydrocarbons saturated the reservoir, it would be more likely concentrated in coarser-grained metasandstones.

Thus, we suggest that the studied object is a metamorphosed oil system consisting of layering oil-source and oil-bearing rocks, with the highest concentration of organic matter in the fine-grained metasedimentary carbonaceous formations.

The presence of the pre-Jurassic weathering crust indicates that by the time of the exposure of these

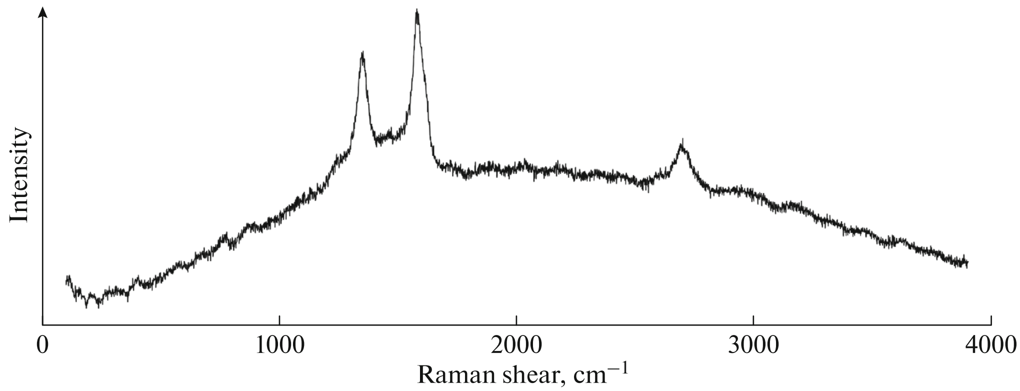

Fig. 7. The Raman shear spectrum for a sample of carbonaceous metasiltstone from well A.

rocks (Triassic or Early Jurassic) the deposit had already been formed and metamorphosed. We can limit the formation of the deposit to the Carboniferous–Triassic time, assuming the Devonian–Carboniferous age of the studied rocks by analogy with the similar rocks of the basement of Em-Egovskaya uplift. If the assumption that the organic matter was transformed due to the contact impact of the massif is correct, this indicates an Early Permian time of metamorphism, because the Kamennyi massif was intruded in the Asselian–Sakmarian time (Ivanov et al., 2018).

The development field of such carbonaceous formations is rather large. According to our data, carbonaceous sericite–quartz shales with interlayers of sandstones and less frequently carbonates are encountered in the basement of the Em-Egovskaya uplift, the eastern slope of the Kamennaya unlift, the Vodorazdelnyi trough, and the Yelizarovskii trough.

CONCLUSIONS

1. The electrical resistivity in the studied metasedimentary rocks of the Krasnoleninsk arch is controlled by only two parameters. The first is rock porosity, whose influence is related to the filling of pore space with conducting fluids. A significant influence of permeability, as the main parameter of rock fracturing, was not detected: there was almost no change in the resistance level with the growth of K_{per}.

2. A distinct negative relationship between ER and the total content of organic matter (TOC correlation) was detected for the first time. This factor is comparable with the influence of the porosity level: an increase in the TOC content by 0.5% leads to a 1000-fold decrease in resistivity.

3. Anthraxolites in the studied samples have a very high degree of transformation (apocatagenesis) and presumably correspond to the “disordered” graphite structure, due to which such a high electric conductivity of the rocks occurs.

4. The patterns we obtained suggest that, in the described case, the low-resistivity zones of the basement rocks do not occur due to high porosity and water saturation, but due to the presence of conductive highly transformed bitumens. This means that when interpreting the GIS data, it is incorrect to unambiguously determine the low-resistivity intervals in the basement as the zones of crushing or increased fracturing; both the rock composition and the probability of such bituminous impregnation have to be taken into consideration.

5. The studied object is a metamorphosed oil system in metasedimentary formations consisting of the alternation of the oil-source and oil-bearing rocks. The source of the hydrocarbons, now represented by bitumens, was primary organic matter from claystones and siltstones, which are now manifested as metaclaystones and metasiltstones. The transformation of organic matter probably occurred as a result of contact metamorphism at the boundary with the Kamennyi intrusive massif.

ACKNOWLEDGMENTS

The authors are grateful to D.A. Ksenofontov, V.S. Shcherbakov, and A.Yu. Bychkov (Moscow State University) for discussion of the problematic issues of the study and assistance in analyzing the results, and to I.A. Mel’nik (School of Earth Science and Engineering, Tomsk Polytechnical University, Tomsk) for providing the authors' articles on the research topic.

FUNDING

This work was performed using equipment purchased with funds from the Development Program of Moscow State University.

REFERENCES

Batalin, O.Yu. and Vafina, N.G., Forms of free-hydrocarbon capture by kerogen, *Mezhd. Zh. Prikladn. Fundamental. Issled.*, 2013, no. 10, pp. 418–425.

Bochkarev, V.S. and Brekhuntsov, A.M., The tectonic scheme of the Urals–Siberian Region, *Gorn. Vedomosti*, 2015, no. 10, pp. 6–39.

Bochkarev, V.S., Brekhuntsov, A.M., Chuvashov, B.I., et al., New U–Pb zircon ages of rhyolites of the Tura series: Evidence for change of crustal geodynamic regimes in the Uralides, *Gorn. Vedomosti*, 2013, no. 3, pp. 6–28.

Chuvashov, B.I., Bochkarev, V.S., and Brekhuntsov, A.M., The Marine Devonian in the Northern Part of Western Siberia, *Dokl. Earth Sci.*, 2009, vol. 429, no. 1, pp. 1295–1298.

Ezhova, A.V., Methods of estimation of oil saturation of low-ohm collectors in Jurassic depositions of South-East of Western Siberian platform, *Izv. Tomsk. Politekhn. Univ.*, 2006, vol. 309, no. 6, pp. 23–26.

Fedorov, Yu.N., Ivanov, K.S., Erokhin, Yu.V., et al., Granitoids of the Uralian part of Western Siberia, *Gorn. Vedomosti*, 2006, no. 12, pp. 32–49.

Filippov, M.M., Antraksolity (Anthraxolites), St. Petersburg: FGUP "VNIGRI", 2013.

Gusev, S.I., Analysis of the reasons for low resistivity of productive reservoirs, *Neftepromyslovoe Delo*, 2016, no. 5, pp. 36–40.

Ivanov, K.S., Erokhin, Yu.V., and Ponomarev, V.S., Age and composition of granitoids from the basement of Krasnoleninsky oil and gas region (Western Siberia), *Izv. UGGU*, 2018, vol. 2, no. 50, pp. 7–14.

Khotylev, A.O., Maiorov, A.A., Khudolei, A.K., et al., Granitoid Massifs of the Krasnoleninsky Arch in Western Siberia: Composition, Structure, Age, and Formation Conditions, *Geotectonics*, 2021, vol. 55, no. 2, pp. 219–239.

Kozlova, E.V., Fadeeva, N.P., Kalmykov, G.A., et al., Geochemical technique of organic matter research in deposits enriched in kerogen (the Bazhenov Formation, West Siberia), *Moscow. Univ. Geol. Bull.*, 2015, vol. 70, no. 6, pp. 409–418.

Lafargue, E., Espitalie, J., Marquis, F., and Pillot, D., Rock-Eval 6 application in hydrocarbon exploration, production and in soil contamination studies, *Rev. Inst. Francais Petrol.*, 1994, vol. 53, no. 4, pp. 421–437.

Lopatin, N.P. and Emets, T.P., *Piroliz v neftegazovoi geologii* (Pyrolysis in Petroleum Geology), Moscow: Nauka, 1987.

Mel'nik, I.A. and Erofeev, L.Ya., Physical-geochemical model of a low-resistance collector and its practical application, *Geol. Modelirovanie*, 2014, no. 3, pp. 46–50.

Mel'nik, I.A., Reasons for formation of low-resistivity oil-saturated reservoirs, *Geol. Nefti Gaza*, 2018, no. 6, pp. 33–40.

Melenevskii, V.N., Borisova, L.S., and Timoshina, I.D., Pyrolytic characteristics of hard bitumen of kerite–anthraxolite series, *Geol. Nefti Gaza*, 2008, no. 4, pp. 40–45.

Reich, S. and Thomsen, C., Raman spectroscopy of graphite, *Philos. Trans. R. Soc., A*, 2004, vol. 362 (1824), pp. 2271–2288.

Semenov, V.V., Mel'nik, I.A., Pitkevich, V.T., et al., The study of low-resistivity reservoir using core material data, *Geofizika*, 2006, no. 2, pp. 42–47.

Shadrina, S.V., Composition, structure, and age of the pre-Jurassic basement rocks in the northeastern framing of the Krasnoleninsky anticlinal fold, *Oil Gas Geol.*, 2018, no. 4, pp. 27–33.
doi 10.31087-0016-7894-2018-4-27-33

Shadrina, S.V. and Kondakov, A.P., New data on the basement of the northeastern frame of the Krasnoleninsk swell, *Geol. Geologo-Razved. Raboty*, 2014, no. 11, pp. 94–99.

Shungity Karelii i puti ikh kompleksnogo ispol'zovaniya (Karelian Shungites and Their Integrated Use) Sokolov, V. A, Kalinin, Yu. A, Ed., Petrozavodsk, 1975.

Skvortsov, M.B., Dakhnova, M.V., Kopilevich, E.A., et al., Methodological approaches to evaluation of oil resources in the Bazhenov Formation, in *GEOEVRAZIYa-2018. Sovremennye metody izucheniya i osvoeniya nedr Evrazii* (GEOEURASIA-2018: Modern Methods of Research and Exploitation of Interior Part of Eurasia), Moscow, 2018, pp. 120–124.

Surkov, V.S. and Zhero, O.G., *Fundament i razvitie platformennogo chekhla Zapadno-Sibirskoi plity* (Basement and Evolution of the Platform Cover of the West Siberian Plate), Moscow: Nedra, 1981.

Tugareva, A.V., Moroz, M.L., Chernova, G.A., and Belova, E.V., Granitoid magmatism in the Frolov megadepression of the Western Siberia, *Izv. Vyssh. Uchebn. Zaved., Neft' Gaz*, 2018, no. 6, pp. 33–40. .
https://doi.org/10.31660/0445-0108-2018-6-33-44

Western Siberia, in *Geologiya i poleznye iskopaemye Rossii. T. 2* (Geology and Mineral Resources of Russia. Vol. 2), Kontorovich, A.E. and Surkov, V.S., Eds., St. Petersburg: Vseross. Nauchno-Issled. Geol. Inst., 2000.

Translated by V. Krutikova